Integration of scale-down experimentation and general rate modelling to predict manufacturing scale chromatographic separations

Spyridon Gerontas [a], Magnus Asplund [b], Rolf Hjorth [b], Daniel G. Bracewell [a],*

[a] The Advanced Centre for Biochemical Engineering, Department of Biochemical Engineering, University College London, Torrington Place, London WC1 7JE, UK
[b] GE Healthcare, Bio-Sciences AB, SE-751 84 Uppsala, Sweden

ARTICLE INFO

ABSTRACT

Chromatography is an essential downstream processing step in the production of biopharmaceuticals. Here we present an approach to chromatography scale-up using scale-down experimentation integrated with general rate modelling. This type of modelling takes account all contributions to the mass transfer kinetics providing process understanding. The model is calibrated using a 2.5 cm height, 1 ml column and used to predict chromatograms for 20 cm height columns from 40 ml to 160 L volume. Simulations were found to be in good agreement with experimental results. The envisaged approach could potentially reduce the number of experiments, shorten development time and reduce costs.

© 2010 Elsevier B.V. All rights reserved.

1. Introduction

In a maturing industry, cost of production has the attention of management and science. An essential step of downstream processing is chromatography as it offers high selectivity and productivity. Therefore the economic design and optimisation of a new chromatography operation is critical.

The sector is currently engaged in applying Quality by Design (QbD) principles to improve process design and to enable this, demonstration of process understanding by small scale experimentation is encouraged [1]. The QbD approach is a systematic route to pharmaceutical development intended to provide guidance to reviewers and investigators on product and process understanding as well as on process control based on sound science and quality risk management. The related ICH guideline encourages gathering of data demonstrating process understanding to be conducted at any scale, but the applicant should justify the relevance of the small or pilot scale to the manufacturing scale and discuss the potential risks of scale-up [1,2].

Chromatography related scale-down studies are typically developed with milligram quantities of product, ideally providing information to produce many tens of kilograms per year if the product is a clinical success [3]. Specifically, scale-down columns (~2.5 cm height, 1 ml) are used to screen for different matrices and mobile phase compositions in order to find working conditions for further development in standard laboratory scale columns at full bed height (~20 cm height, 40 ml). Scale-up strategies suggested in literature and used currently in industry are based on keeping the column height and the linear velocity constant through transition from laboratory to manufacturing scale. Such approaches make scale-up time consuming and expensive as they require a substantial amount of material even at the smallest scale [3]. Additionally, the number of early stage experiments is limited and optimisation of the chromatographic steps is delayed until late on in development when sufficient amount of feed material is available [4].

The use of scale-down experimentation integrated with rate models based on the underlying physical mechanisms of the separation process make it possible to use the data to demonstrate process understanding up to manufacturing scale. Such models can be used as a predictive tool over a wider range of operating conditions, resin types and column dimensions than empirical based models. This will reduce the number of laboratory intensive experiments and thereby shorten development time and reduce costs.

This paper focuses on the prediction of laboratory and manufacturing scale ion-exchange separations of a protein solution of bovine serum albumin and lactoferrin using data from scale-down experimentation with three resin types. The mathematical model used in this study is the general rate model with mobile phase modulator [5]. It is a comprehensive chromatography model which takes into account intra- and inter-particle mass transport, adsorption/desorption kinetics on the site of the particles and salt-induced elution.

* Corresponding author. Tel.: +44 (0)20 7679 2374; fax: +44 (0)20 7209 0703.
E-mail address: d.bracewell@ucl.ac.uk (D.G. Bracewell).

Binding parameters for the proteins are estimated from the chromatograms of 1 ml columns using the inverse method [6]. Analytically, the values of the binding parameters are changed in an iterative way until the squared differences between the experimental and simulated values are minimised [7–14]. Laboratory and manufacturing scale chromatographic separations were predicted using binding parameters calculated from the small scale and were validated against experimentally obtained chromatograms.

2. Materials and methods

2.1. Materials

Unless stated otherwise, materials were supplied by GE Healthcare, Uppsala, Sweden. Scale-down chromatography was conducted using HiTrap^{TM} columns connected to an ÄKTApurifier^{TM} system (Table 1). The columns were pre-packed with SP Sepharose^{TM} Fast Flow (6% cross-linked agarose, functional group: $-CH_2CH_2CH_2SO_3{}^-$, 90 μm average particle size), Capto^{TM} S (6% cross-linked agarose grafted with 40 kDa dextran, functional group: $-O-CH_2CH_2SO_3{}^-$, 90 μm average particle size) and SP Sepharose^{TM} High Performance (6% cross-linked agarose, functional group: $-CH_2CH_2CH_2SO_3{}^-$, 34 μm average particle size). All properties are reported by the manufacturer.

Laboratory scale chromatography was conducted using XK^{TM} 16 columns connected to an ÄKTApurifier^{TM} system (Table 1). The columns were pre-packed with SP Sepharose Fast Flow, Capto S and SP Sepharose High Performance.

In laboratory scale chromatography the dead volume is a significant fraction of the system's total volume and it must be measured in order to correct the obtained experimental elution profiles. In this study the measured dead volume was 0.65 ml (experimental protocol by Hutchinson et al. [4]).

Manufacturing scale chromatography was conducted using AxiChrom^{TM} columns connected to an ÄKTApilot^{TM} or ÄKTAprocess^{TM} system. Specifically, AxiChrom 400 and AxiChrom 1000 were packed with SP Sepharose Fast Flow whereas AxiChrom 70 and AxiChrom 600 were packed with Capto S. Buffers and sample were prepared in large containers and then divided to the four columns which were run in parallel on four different ÄKTAprocess^{TM} systems.

Bed efficiency test was conducted by equilibrating the columns for three column volumes before 0.01 column volumes of 2% v/v acetone in ultrapure water was applied to the bed. The acetone was eluted at 30 cm h^{-1}.

All columns satisfied the acceptance criteria for reduced plate height (<3) and asymmetry factor (<1.3) (Table 1). The protein solution contained bovine serum albumin (BSA)-molecular weight: 67 kDa, isoelectric point: 4.8 (Serologicals Corp., Georgia, USA) and lactoferrin – molecular weight: 82 kDa, isoelectric point: 8.8 (Arla Foods, UK plc, Leeds, UK) All chemicals were of analytical grade and their properties are reported by the manufacturer. Table 1 summarises resins, columns and chromatography systems used.

2.2. Column packing

2.2.1. AxiChrom 400, 600 and 1000 columns

Packing was performed using an ÄKTAprocess^{TM} chromatography system and an AxiChrom Master column controlling unit. The packing procedure was controlled automatically according to pre-set parameters. After priming the column and slurry hose with 20% ethanol, homogenous slurry (in 20% ethanol) with known concentration (65% gravity settled bed volume/slurry volume) and volume was sucked into the column by raising the adaptor at 300 cm h^{-1}. The slurry valve was then closed and the slurry hose

Table 1
Summary of some basic materials and experimental conditions.

Column	Diameter (mm)	Bed height (cm)	Volume (L)	SP Sepharose High Performance		SP Sepharose Fast Flow		Capto S		Chromatography system	Piping diameter (mm)
				A_s	HETP (cm)	A_s	HETP (cm)	A_s	HETP (cm)		
HiTrap	7	2.5	0.001	1.3	0.009	1.2	0.023	1.2	0.024	ÄKTApurifier	0.75
XK	16	19.9	0.040	1.1	0.014	1.1	0.021	1.1	0.020	ÄKTApurifier	0.75
AxiChrom	70	19.6	0.754					1.4	0.020	ÄKTApilot	2.9
AxiChrom	400	19.5	24.5			1.1	0.013			ÄKTAprocess	10.0
AxiChrom	600	19.8	56.0					1.1	0.027	ÄKTAprocess	10.0
AxiChrom	1000	19.5	153			1.1	0.013			ÄKTAprocess	25.0

Table 2
Separation conditions on SP Sepharose Fast Flow runs.

SP Sepharose FF	Fluid velocity (cm h^{-1})	Bovine serum albumin (BSA)		Lactoferrin	
		Experimental elution conductivity[a] (mS cm^{-1})	Theoretical elution conductivity[a] (mS cm^{-1})	Experimental elution conductivity[a] (mS cm^{-1})	Theoretical elution conductivity[a] (mS cm^{-1})
HiTrap	50	38.6	38.4	83.6	84.3
XK16	100	38.8	39.3	74.8	74.1
AxiChrom 70	100	31.2	26.9	76.4	77.2
AxiChrom 400	100	38.9	39.3	84.7	84.8
AxiChrom 1000	100	37.8	38.5	74.5	75.8

[a] Peak.

was rinsed from resin. The mobile phase valve in the bottom of the column was opened and the adaptor was driven downwards at 60 cm h^{-1} to pack the bed based on the packing factor (PF) 1.15, calculated from the consolidated bed. PF is defined as consolidated bed height/packed bed height, where the consolidated bed height is read when the adapter reaches the consolidated bed (a bed exposed to an external force, e.g. a flow) and the packed bed height is read when the bed has been mechanically compressed to its final position.

2.2.2. AxiChrom 70 column

Packing was performed using an ÄKTApilot^{TM} chromatography system. The packing procedure was controlled by UNICORN^{TM} software according to pre-set parameters. To prepare the column for packing, the bottom bed support was purged from air by pumping 20% ethanol through the bottom inlet until approximately 1 cm of liquid was seen above the bed support. With the bottom inlet still connected to the system, homogenous gel slurry (in 20% ethanol) (65% gravity settled bed volume/slurry volume) was poured into the column. Packing buffer was then filled up to the edge of the glass tube. Held upside down the adapter was primed with packing buffer. The gel slurry was stirred up and down using a plastic stirrer to become homogenous. It was thereafter allowed to sediment by gravity until a clear liquid phase 2 cm high was seen in the upper part of the column before the adapter was mounted. The bed was packed to a packing factor (PF) 1.15 by lowering the adaptor at 60 cm h^{-1}.

2.3. Protocols

2.3.1. Scale-down chromatography protocols

2.3.1.1. SP Sepharose High Performance and SP Sepharose Fast Flow. HiTrap SP Sepharose High Performance and SP Sepharose Fast Flow columns were equilibrated with seven column volumes of start buffer composed of 50 mM acetic acid, pH 4.5. A protein sample, 1 ml was loaded to the HiTrap column at the desired linear velocities (Tables 2–4). The mass ratio of BSA to lactoferrin was 3:1 with the load of the total protein to be 4.2 mg per ml of resin. The columns were washed with two column volumes of start buffer at the same

fluid velocity. Gradient elution was performed by increasing the concentration of the elution buffer composed of 50 mM acetate and 1 M NaCl, pH 4.5 from 0% to 100% over 10 column volumes at variable linear velocities and washed with two column volumes elution buffer. The columns were then re-equilibrated at the same fluid velocity with three column volumes of start buffer.

2.3.1.2. Capto S. HiTrap Capto S columns were equilibrated with 10 column volumes of start buffer containing 50 mM sodium acetate pH 5. A protein sample, 1 ml, was loaded at the desired fluid velocity (Table 2). The total protein was 2 mg ml^{-1} of resin in 1:1 mass ratio. The columns were washed with 5 column volumes of start buffer at the same fluid velocity. Gradient elution was performed by increasing the concentration of the elution buffer composed of 50 mM acetate and 1 M NaCl, pH 5 from 0% to 100% over 20 column volumes at the same fluid velocity. The columns were then re-equilibrated at the same fluid velocity with five column volumes of start buffer.

2.3.2. Laboratory scale chromatography protocol

The laboratory scale experiments were conducted under the protocols followed in the scale-down experiments. The sample volume was 20 ml and 15.6 ml for the Capto S and SP Sepharose High Performance/SP Sepharose Fast Flow runs respectively. The total protein concentration was 4 mg ml^{-1} and 10 mg ml^{-1} for the Capto S and SP Sepharose HP/FF runs respectively. The mass ratios of BSA to lactoferrin were equal to the ones used in scale-down experiments.

2.3.3. Manufacturing scale chromatography protocol

Manufacturing scale experiments were conducted under the protocols followed in the scale-down experiments. The sample volume was one column volume and 0.4 column volumes for the Capto S and SP Sepharose High Performance/SP Sepharose Fast Flow runs respectively. The total protein concentration was 4 mg ml^{-1} and 10 mg ml^{-1} for the Capto S and SP Sepharose HP/FF runs respectively. The mass ratios of BSA to lactoferrin were equal to the ones used in the scale-down experiments.

Table 3
Separation conditions on Capto S runs.

Capto S	Fluid velocity (cm h^{-1})	Bovine serum albumin (BSA)		Lactoferrin	
		Experimental elution conductivity[a] (mS cm^{-1})	Theoretical elution conductivity[a] (mS cm^{-1})	Experimental elution conductivity[a] (mS cm^{-1})	Theoretical elution conductivity[a] (mS cm^{-1})
HiTrap	78	9.4	10.6	51.7	53.1
	156	9.3	10.1	52.1	53.9
XK16	156	10.2	10.8	53.6	52.9
	312	10.3	10.1	53.5	55.1
AxiChrom 70	50	8.0	8.2	42.1	41.3
AxiChrom 600	50	10.8	10.7	48.1	48.1

[a] Peak.

Table 4
Separation conditions on SP Sepharose High Performance runs.

SP Sepharose HP	Fluid velocity (cm h^{-1})	Bovine Serum Albumin (BSA)		Lactoferrin	
		Experimental elution conductivity[a] (mS cm^{-1})	Theoretical elution conductivity[a] (mS cm^{-1})	Experimental elution conductivity[a] (mS cm^{-1})	Theoretical elution conductivity[a] (mS cm^{-1})
HiTrap	13	37.0	36.8	102.7	102.6
	50	40.8	45.7	101.5	100.7
	100	43.4	45.0	101.7	101.8
XK16	50	37.9	39.0	105.9	105.8
	75	37.9	38.8	105.8	109.7
	100	38.7	41.3	105.9	105.4

[a] Peak.

2.4. Absorbance – conductivity

The loading, washing and elution step was monitored by detecting absorbance at 280 nm and conductivity (mS cm^{-1}). The total absorbance was assumed to be additive for the components included in the simulation. The concentration was converted into absorbance using standard curves obtained for each protein. The conversion factor for BSA and lactoferrin were 0.14 AU ml mg^{-1} and 0.38 AU ml mg^{-1} respectively.

The injected BSA concentration was adjusted in the model as the tailing in the BSA's elution profile was not considered when fitting the model to the experimental data. This adjustment was made according to the work of Suda et al. [15]. Specifically, they have shown using size exclusion chromatography and SDS-PAGE that the tailing is attributed to BSA aggregates which are present in the feed material and composed primarily of dimeric species. These aggregates comprise 11.7% of the total mass of BSA, while monomer comprises 87.2% [15].

3. Theory/calculation

3.1. Mathematical model

The general rate model with mobile phase modulator was used to simulate the elution profiles. It takes into account axial dispersion, resistance to film mass transfer, intra-particle diffusion, adsorption/desorption kinetics and salt-induced elution [5]. It contains one partial differential equation to describe mass transfer in the mobile phase, one partial differential equation to describe mass transfer in the beads and one ordinary differential equation to describe the adsorption/desorption kinetics.

The adsorption/desorption kinetics are described by Langmuir kinetics with mobile phase modulator. In this description adsorption competes with desorption and the protein retention is controlled by the salt concentration. The salt is considered to be inert and it is not adsorbed in the solid phase of the resin.

The model has the following assumptions: (i) the chromatographic separation is isothermal, (ii) the chromatographic columns are evenly packed with spherical, porous beads of uniform size, (iv) there is no variation in the protein concentration in the direction perpendicular to the direction of the flow (no radial concentration gradient), (v) the velocity profile is flat, (vi) the physical properties of the particle are constant and independent of the protein/salt concentration, (vii) the mass transfer within the beads is controlled by diffusion, (viii) the mass transfer parameters are concentration independent parameters and (ix) the salt is inert.

The equation which describes the mass transfer of proteins and salt in the mobile phase is solved on the axial coordinate (which is parallel to the direction of the flow) as it has been assumed that there is no variation in concentration in the direction perpendicular to the direction of the flow. The differential mass balance in the bulk liquid phase is described by:

$$\frac{\partial c_{bi}}{\partial t} + v_{int}\frac{\partial c_{bi}}{\partial z} = D_{ax}\frac{\partial^2 c_{bi}}{\partial^2 z} - \frac{3k_i(1-\varepsilon_b)}{\varepsilon_b R_p}(c_{bi} - c_{pi,r=R_p}) \tag{1}$$

where c_{bi} is the concentration of component i in the mobile phase, t is the time, v_{int} is the interstitial velocity, z is the axial coordinate, D_{ax} is the dispersion coefficient, k_i is the film mass transfer coefficient for the component i, ε_b is the bed void volume fraction, R_p is the average bead radius, $c_{pi,r=R_p}$ is the concentration of component at the surface of the bead, $\partial c_{bi}/\partial t$ is the accumulation rate of component i per unit volume in the liquid phase of the column, $-3k_i(1-\varepsilon_b)(c_{bi}-c_{pi,r=R_p})/\varepsilon_b R_p$ is the amount of component i which is transferred from the mobile phase to the surface of the particle, the remainder of the left hand side of the equation represents the rate per unit volume of mass transfer by convection and of the right hand side represents the rate per unit volume of mass transfer by dispersion.

The boundary conditions for Eq. (1) are the following:
At the inlet of column:

$$\frac{\partial c_{bi}}{\partial z} = \frac{v_{int}}{D_{ax}}(c_{bi} - c_{bi,inlet}), z = 0 \tag{2}$$

where $c_{bi,inlet}$ is the inlet concentration. The latter can be lower than the feed inlet concentration due to dispersion at the inlet of the column.

At the outlet of the column, only convective transport is considered:

$$\frac{\partial c_{bi}}{\partial z} = 0, z = L \tag{3}$$

where L is the length of the column. The equation which describes the differential mass balance of proteins and salt in the bead is the following:

$$(1-\varepsilon_p)\frac{\partial q}{\partial t} + \varepsilon_p\frac{\partial c_{pi}}{\partial t} = \varepsilon_p D_{pi}\left(\frac{1}{r^2}\frac{\partial}{\partial r}\left(r^2\frac{\partial c_{pi}}{\partial r}\right)\right) \tag{4}$$

where r is the radial coordinate, ε_p is the accessible particle void fraction, q is the concentration of the component i in the solid phase of the absorbents based on the unit volume of the solid, excluding pores, D_{pi} is the molecular diffusivity of component i in the liquid phase of the beads, c_{pi} is the concentration of the component i in the liquid phase inside the beads, $\partial c_{bi}/\partial t$ is the accumulation rate per unit volume of component i in the liquid phase of the bead, $\partial q/\partial t$ is the accumulation of component i in the solid phase of the bead and the remainder of the left hand side of the equation represents the rate per unit volume of mass transfer by diffusion in the liquid phase of the bead.

The boundary conditions for Eq. (4) are the following:
At the surface of the bead:

$$\frac{\partial c_{pi}}{\partial r} = \frac{k_i}{\varepsilon_p D_{pi}}(c_{bi} - c_{pi,r=R_p}), \quad r = R_p \tag{5}$$

At the centre of the bead:

$$\frac{\partial c_{pi}}{\partial r} = 0, \quad r = 0 \tag{6}$$

Adsorption/desorption of the proteins in the beads is described by Langmuir kinetics with a phase modulator. It is expressed mathematically as follows:

$$\frac{\partial q_i}{\partial t} = k_{ads,i}c_i(q_{max,i} - q_i) - k_{des}q_i \tag{7}$$

where q_i is the concentration of component i in the stationary phase, $q_{max,i}$ is the maximum concentration of component i in the stationary phase, $k_{ads,i}$ is the adsorption coefficient and $k_{des,i}$ is desorption coefficient.

The parameters $k_{ads,i}$ and $k_{des,i}$ are expressed mathematically as a function of the salt concentration of the gradient elution buffer (phase modulator) as follows:

$$k_{ads,i} = k_{ads0,i}e^{\gamma iS} \tag{8}$$

$$k_{des,i} = k_{des0,i}S^{\beta_i} \tag{9}$$

where S is the concentration of the salt in the elution buffer, $k_{ads0,i}$, $k_{des0,i}$ are constants, β_i is a constant which characterises the ion-exchange and γ_i is a constant which characterise hydrophobic interactions. Hydrophobic interactions are considered negligible thus γ_i is considered to be equal to zero. A linear relationship between the salt concentration and the conductivity of the start and elution buffer has been assumed. The initial salt concentration in the column is 0.02 M.

There is no protein initially present in the column therefore:

$$c_{pi} = c_{pi}(0, Z) = 0 \tag{10}$$

$$c_{bi} = c_{bi}(0, R) = 0 \tag{11}$$

$$q_i = q_i(0, R) = 0 \tag{12}$$

The bed void fraction for SP Sepharose has been reported to be in the range of 0.29–0.42 [16]. The value of 0.35 was used in the mathematical model. The axial dispersion D_{ax} was estimated from the following equations [17]:

$$D_{ax} = \frac{v_{int}L}{Pe} \tag{13}$$

$$Pe = \frac{0.1L}{R_p\varepsilon_b} \tag{14}$$

where Pe is the Peclet number.

Additionally, the film mass transfer coefficient is calculated from the correlation of Wilson and Geankoplis [18]:

$$k_i = 0.687v_{int}^{\frac{1}{3}}\left(\frac{R_p\varepsilon_b}{D_M}\right)^{-\frac{2}{3}} \tag{15}$$

The molecular diffusivity of proteins in water D_M was calculated from the correlation of Polson [19]:

$$D_M = 2.74 \times 10^{-5}M^{-1/3} \tag{16}$$

where M is the molecular weight of the protein. The above equations neglect wall effect phenomena. There are valid when the ratio of the diameter of the column to the average diameter of the bead is above 30 [20]. This ratio for HiTrap columns (smallest columns used in this study; 0.7 cm diameter) packed with SP Sepharose Fast Flow/Capto S resins (90 μm average bead diameter) is around 78 and it is around 206 when they are packed with SP Sepharose HP (34 μm average bead diameter).

The accessible particle void fraction of SP Sepharose and Capto S was set to 0.62 and 0.37 respectively [21]. This difference has been attributed to the presence of dextran coating in Capto S resin [21].

Table 5
Bounds for parameter estimation.

Parameter	Lower limit	Upper limit	Refs.
$q_{max,i}$[b] (mg ml^{-1})	0	800[a]	[21]
$k_{ads,i}$[b] (ml mg^{-1} s^{-1})	0	0.3[a]	[22]
$k_{des0,i}$[b] (ml mg^{-1} s^{-1})	0	0.5[a]	[21–23]
β (−)	0	6[a]	[9]
D_{pi} (10^{-7} cm^2 s^{-1})	0	protein diffusivity in water	[19]

[a] Set at twice the reported value.
[b] Expressed in terms of hydrated bead volume (solid bead volume/$(1 - \varepsilon_p)$).

3.2. Numerical method

The finite element method implemented in Comsol Multiphysics™ 3.4 (Comsol Ltd., Hatfield, UK) was used to discretize the system of differential equations. The bead is spherically symmetric therefore the mass transfer equations for the bead can be expressed in 1D spherical coordinates. At each distance from the entrance of the column a single 1D model, representative of all beads at this distance is modelled. By joining all the 1D bead models along the length of column a 2D geometry is generated. The column can be modelled in the same 2D geometry like the beads by cancelling out the radial coordinate (no radial concentration gradient). The column is rotationally symmetric due to its cylindrical shape, thus it is possible to be modelled in cylindrical coordinates. The bead model is coupled to the column model by exporting the protein concentration at the surface of the bead and inserting it to the mass transfer equation for the column. Similarly, the protein concentration in the mobile phase of the column is inserted in the surface boundary condition of the bead. In all simulations, the number of grid points in the radial and axial coordinate was set to 10 and 400 respectively. The convergence was tested by increasing the number of elements by two orders of magnitude. The protein concentrations simulated using the new mesh were in agreement at the three significant figures level with the default mesh used in the chromatography simulations.

3.3. Inverse method

The model was calibrated using the elution profile of the protein sample in 1 ml HiTrap columns. The inverse method is applied in two steps using Comsol Multiphysics wrapped around Matlab™ (The MathWorks Inc., Natick, USA). In the first step the Comsol model is developed in Comsol's graphical user interface using arbitrary values for the parameters of interest. It is then saved as a Matlab file. In this form the file can run in Matlab's graphical user interface without the option to alter the values of the parameters of interest and calibrate the model to experimental data. This is achieved by editing the file as a Matlab function so as to treat the system of differential equations of the model as a functional representation between the parameters of interest which are the input and the sum of squared residuals (a residual is defined as the difference between the experimental and the fitted value) which is the output. This Matlab function is referred to as the forward model function. Its role is to help Matlab recognise which parameters of the Comsol model need to be estimated. In the second step the genetic algorithm Matlab function "ga" is used to minimise the forward model function. The genetic algorithm is used to ensure that a global minimum is reached. It searches for optimal parameter values within the range imposed by the upper and lower bounds shown in Table 5, as using it without setting bounds could lead in results without physical meaning. The population size was set to 100 and the rest of the settings were kept to their default values. The poor search precision of the genetic algorithm due to its probabilistic nature is overcome by the use of the derivative-based search Matlab function "fminunc" (default settings). Specifically,
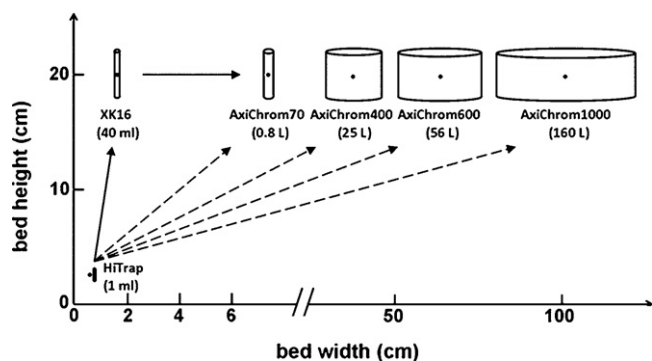
Fig. 1. Schematic to demonstrate the conventional route (solid arrow) versus the proposed route (dotted arrow) of scale-up. In the conventional route scale-down columns (~1 ml) are used to define optimal conditions for laboratory scale columns (~40 ml) which have the same height as manufacturing scale columns (AxiChrom columns). Performance at the manufacturing scale is assessed by running the laboratory scale columns at the same velocity. In the proposed route the scale-down experimentation integrated with mathematical modelling are used for the prediction of the manufacturing scale.

the genetic algorithm finds a point close to the optimal one and then that point is used as an initial guess for "fminunc". The "fminunc" function cannot be used instead of the "ga" function because it is a derivative-based search algorithm and it is often trapped into local optima. The parameter values were estimated in 18 h CPU times on an Intel Dual-Core Pentium Xeon 5160/3 GHz processor with 4 Gb memory. Both cores were under load during simulation and 0.8 Gb out of 4 Gb memory were allocated for Comsol Multiphysics.

4. Results

A comparison between the conventional and the proposed route of scaling-up chromatographic separations is presented in Fig. 1. In the conventional route, small (~2.5 cm height, 1 ml) columns are used to screen different matrices and mobile phase compositions in order to determine a suitable separation. These conditions can then be replicated in full bed height laboratory (~20 cm height, 40 ml) columns where further development of operating variables can take place. Scale-up is then achieved by keeping the column height and the fluid velocity constant through transition from laboratory to manufacturing scale.

In the route proposed in this paper, a model based on the physiochemical mechanisms of chromatographic separation is integrated with scale-down data to predict manufacturing scale. Specifically, we used 1 ml column data to calculate the adsorption/desorption kinetic parameters and effective diffusivity (Table 6) and we challenged the model using the calculated values to predict the laboratory and manufacturing scale separation at different fluid velocities (50–100% increase from 1 ml column), different sample size (from 1 CV in 1 ml column to 0.4 CV in scale-up columns) and different height (from 2.5 cm in 1 ml column to 20 cm in scale-up columns).

The prediction of the elution profile of the BSA and lactoferrin was conducted using three resins: SP Sepharose Fast Flow, Capto S and SP Sepharose High Performance.
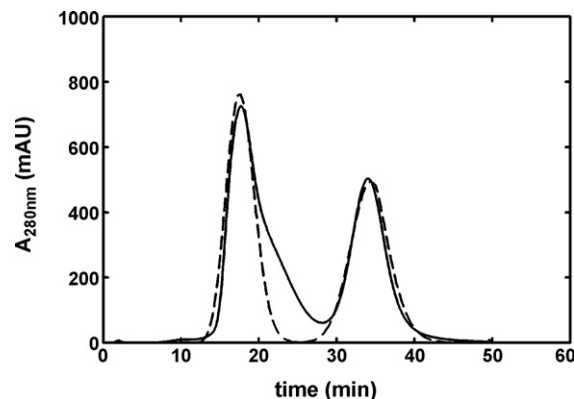

Fig. 2. Experimental (—) and simulated (– – –) chromatograms from a run on a SP Sepharose Fast Flow HiTrap 1 ml column. The general rate model has been used to model loading, washing and gradient elution step of 1 ml protein solution containing 7.5 mg ml^{-1} BSA and 2.5 mg ml^{-1} lactoferrin. Both loading (1 column volume) and washing (2 column volumes) were conducted at 100 cm h^{-1}. The gradient elution was performed at 50 cm h^{-1} by increasing the concentration of the elution buffer from 0% to 100% over 10 column volumes. Following elution the column was washed with 2 column volumes of elution buffer without changing the fluid velocity.

The first resin to be tested was the SP Sepharose Fast Flow as it is well established and widely used in industry. Experimental elution data obtained from 1 ml columns were used to calibrate the general rate model (Fig. 2). This calibration refers to the determination of the maximum capacity of each protein, the parameters of the kinetics of their adsorption/desorption kinetics on the resin and their effective diffusivities in the beads.

The model predicted the elution profile of XK16 and AxiChrom columns by adjusting it to the dimensions of those columns and using the parameters derived from the 1 ml column data (Fig. 3).

The accuracy of the mathematical model in predicting the shape of the elution profile of BSA in laboratory and manufacturing scale from scale-down data is lower than for lactoferrin. Specifically, in all scales of operation there is a tailing in the BSA elution profile which causes displacement of the prediction peak (Fig. 3). These additional components can be added to the model, however in many cases may be unknown and therefore we have chosen this more generic situation which excludes the aggregates.

The experimental elution profiles in Fig. 3 show that the resolution of BSA (without considering the tailing part) and lactoferrin decreases with increasing fluid velocity through the bed. This is expected as the proteins have less time to diffuse through the beads and bind to the resin. It is more noticeable in the 1 ml columns because of their short length and therefore proportionally reduced plate number and residence time for a protein to enter the bead and bind to the resin. Additionally, mass transfer inside the beads is independent of the flow rate as the convection inside them is considered negligible.

Capto S was the next resin to be tested. Calibration of the model is achieved by fitting the model to 1 ml data (Fig. 4) and the prediction of the large scale is presented in Figs. 5 and 6.
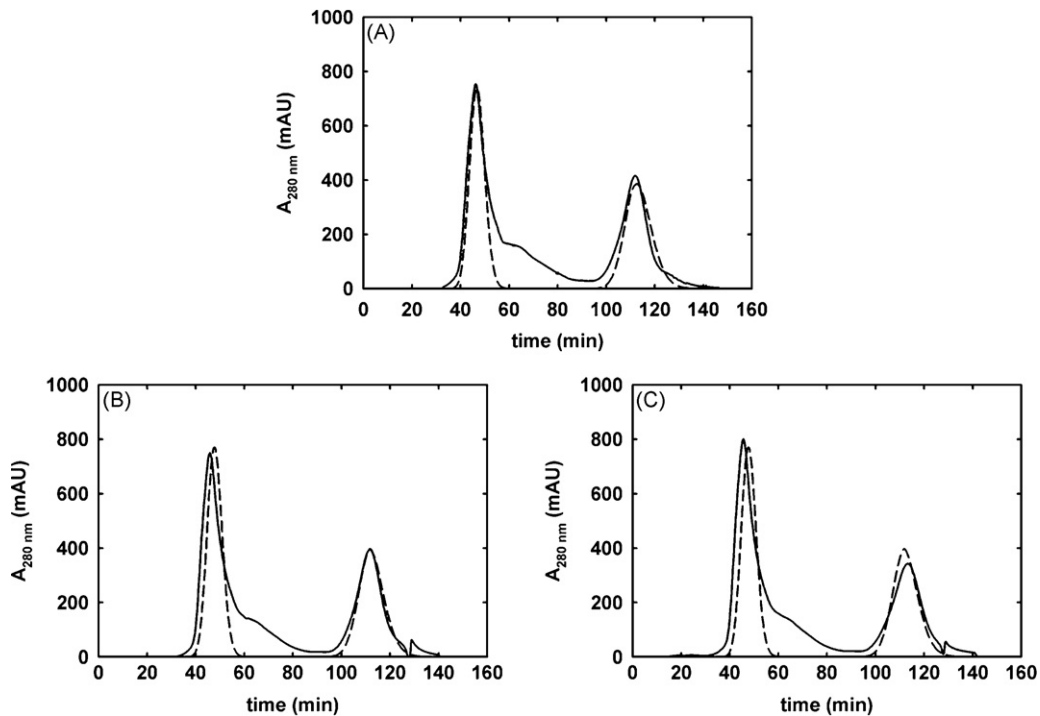
Table 6
Parameter estimations.

Resin	$q_{max,i}$[a] (mg ml^{-1})		$k_{ads,i}$[a] (ml mg^{-1} s^{-1})		$k_{des0,i}$[a] (10^{-3} ml mg^{-1} s^{-1})		β (–)		D_{pi} (10^{-7} cm^2 s^{-1})	
	BSA	LF	BSA	LF	BSA	LF	BSA	LF	BSA	LF
SP Sepharose Fast Flow	182	302	0.19	0.41	117	3.6	4.4	4.2	1.2	1.4
Capto S	205	405	0.29	0.53	83	3.5	2.4	2.9	4.8	3.7
SP Sepharose High Performance	198	254	0.19	0.29	115	3.2	4.8	4.8	1.5	1.2
		302[b]		0.40[b]		3.2[b]		4.3		1.2[b]

[a] Expressed in terms of hydrated bead volume (solid bead volume/($1 - \varepsilon_p$)).
[b] Parameters refer to the larger peak, the other resins do not resolve lactoferrin into two peaks.

Fig. 3. Validation of the calculation of the model parameters through the comparison of experimental (—) and predicted (– – –) chromatograms from runs on Sepharose Fast Flow XK16; 40 ml (A), AxiChrom 400; 25 L (B) and AxiChrom 1000; 160 L (C) columns. The elution profiles are obtained by loading the columns with 0.4 column volume of a protein solution containing 7.5 mg ml^{-1} BSA and 2.5 mg ml^{-1} lactoferrin, washing them with 2 column volumes and eluting them by increasing the concentration of the elution buffer from 0% to 100% over 10 column volumes. Following elution the columns were washed with 2 column volumes of elution buffer without changing the fluid velocity. In all cases the columns were loaded and washed at 150 cm h^{-1} whereas they were eluted at 100 cm h^{-1}. The values of model parameters have been calculated from the chromatogram in Fig. 2.
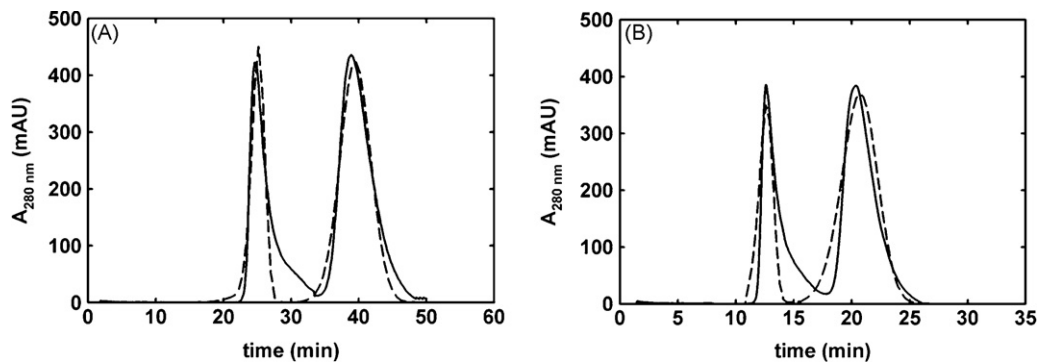
Fig. 4. Experimental (—) and simulated (– – –) chromatograms from runs on Capto S HiTrap 1 ml columns. The loading (1 column volume), washing (2 column volumes) and gradient elution step of 1 ml protein solution containing 1.0 mg ml^{-1} BSA and 1.0 mg ml^{-1} lactoferrin were conducted at 78 cm h^{-1} (A) and 156 cm h^{-1} (B). Gradient elution was performed by increasing the concentration of the elution buffer from 0% to 100% over 20 column volumes. Following elution the column was washed with 5 column volumes of elution buffer without changing the fluid velocity.
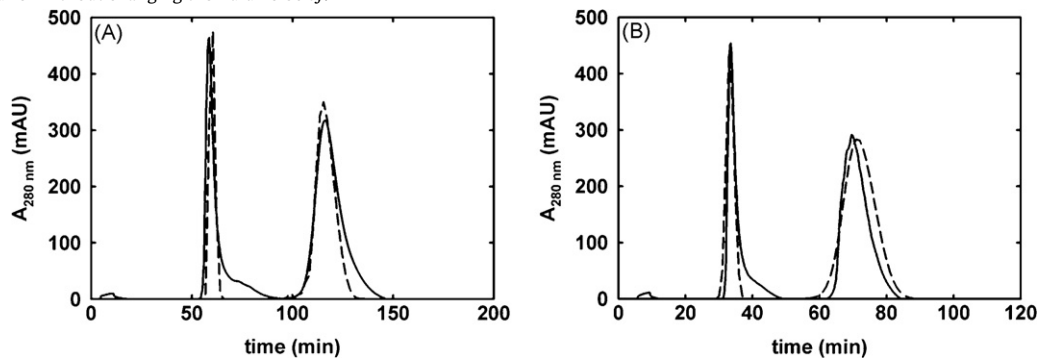
Fig. 5. Validation of the calculation of the model parameters through the comparison of experimental (—) and predicted (– – –) chromatograms from runs on Capto S XK16; 40 ml laboratory columns. The elution profiles of a protein solution containing 2.0 mg ml^{-1} BSA and 2.0 mg ml^{-1} lactoferrin are obtained by loading the column with 0.5 column volumes, washing it with 5 column volumes, and eluting by increasing the concentration of the elution buffer from 0% to 100% over 20 column volumes. Following elution the column was washed with 5 column volumes of elution buffer without changing the fluid velocity. The column was loaded, washed and eluted at 156 cm h^{-1} (A) and 312 cm h^{-1} (B). The values of model parameters have been calculated from the chromatogram in Fig. 4.
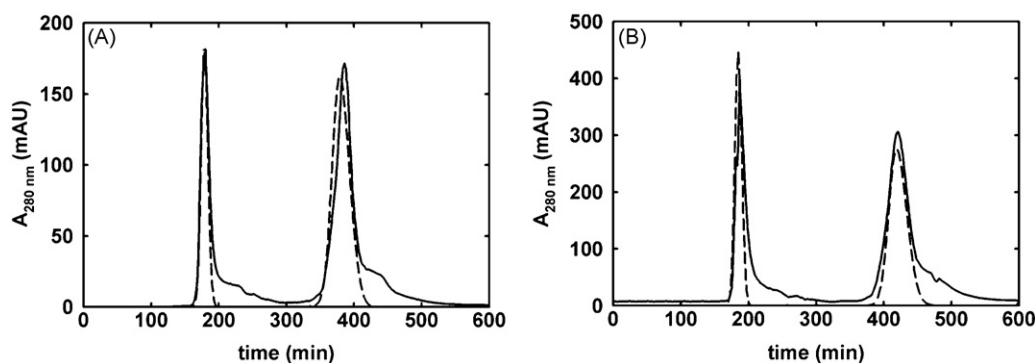
Fig. 6. Validation of the calculation of the model parameters through the comparison of experimental (—) and predicted (– – –) chromatograms from runs on Capto S AxiChrom 70; 0.75 L (A) and AxiChrom 600; 56 L (B) columns. The elution profiles of protein solutions containing 1.0 mg ml^{-1} BSA and 1.0 mg ml^{-1} lactoferrin (AxiChrom 70) and 2.0 mg ml^{-1} BSA and 2.0 mg ml^{-1} lactoferrin (AxiChrom 600) are obtained by loading the columns with 0.5 column volumes, washing them with 5 column volumes and eluting them by increasing the concentration of the elution buffer from 0% to 100% over 20 column volumes. Following elution the columns were washed with 5 column volumes of elution buffer without changing the fluid velocity. In both cases the columns were loaded, washed and eluted at 50 cm h^{-1}. The values of model parameters have been calculated from the chromatogram in Fig. 4.

Through the use of the model the performance of the resins can be analysed to develop process understanding. Specifically, the maximum capacity and the adsorption coefficient for lactoferrin in Capto S resin were around 30% higher than in the other two resins (Table 6). This has been reported to be a result of surface grafting dextran polymers into Capto S resin's macroporous, cross-linked agarose structure which offers more active sites for binding and enhances surface diffusion [21,24,25].

Capto S at pH 5 had a similar BSA capacity with SP Sepharose at pH 4.5 (Table 6). Hubbuch et al. [26] state that at this pH there are a few positive charged groups on the surface of the protein which could explain why the binding capacity is approximately equal on the two different types of adsorbents.

Additionally, the effective diffusivity for both proteins in Capto S was three times higher than in the other two resins (Table 6). It has been shown that dextran grafting can potentially enhance diffusion into the beads through other diffusion mechanisms such as surface diffusion, transport through grafted material and coupling of electrostatic potential with transport/adsorption mechanisms [24,25].

The lactoferrin elution profile contained two peaks when Sepharose High Performance resin is used (Figs. 6–8). The study was expanded to that resin in order to show the feasibility of the method when used with a smaller bead size and consequently higher resolution resin type. The two lactoferrin peaks are attributed to be protein forms containing ferrous and ferric iron [27]. This difference
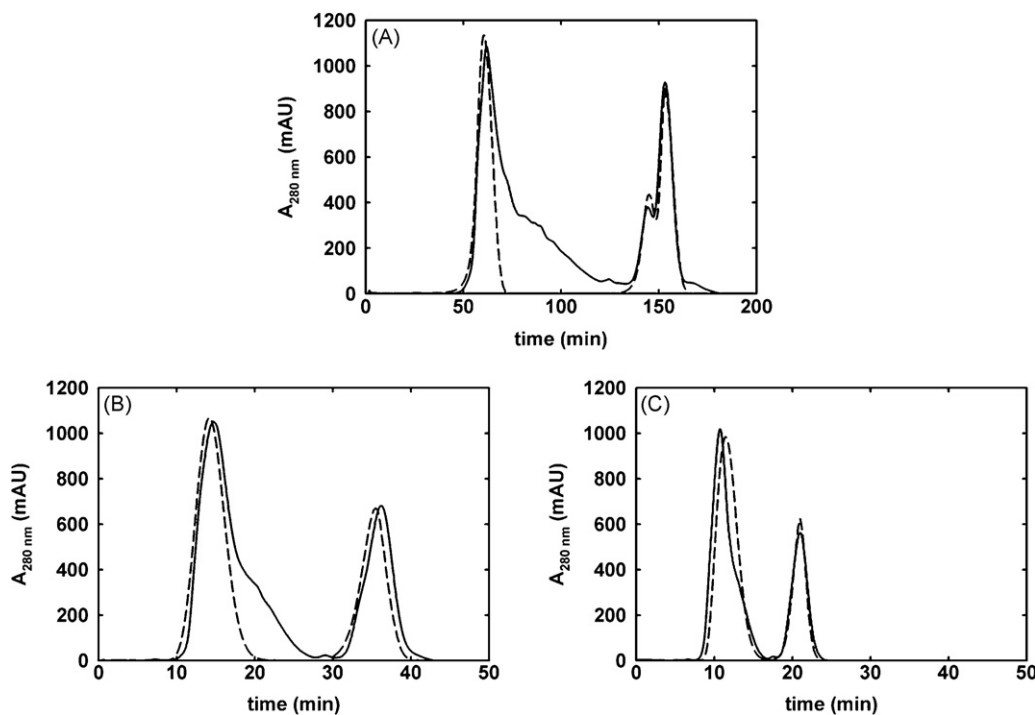

Fig. 7. Experimental (—) and simulated (– – –) chromatograms from runs on SP Sepharose High Performance HiTrap 1 ml columns. The general rate model has been used to model loading, washing and gradient elution step of 1 ml protein solution containing 3.15 mg ml^{-1} BSA and 1.05 mg ml^{-1} lactoferrin. Both loading (1 column volume) and washing (2 column volumes) were conducted at 100 cm h^{-1}. The gradient elution was performed at 13 cm h^{-1} (A), 50 cm h^{-1} (B) and 100 cm h^{-1} (C) by increasing the concentration of the elution buffer from 0% to 100% over 10 column volumes. Following elution the column was washed with 2 column volumes of elution buffer without changing the fluid velocity.
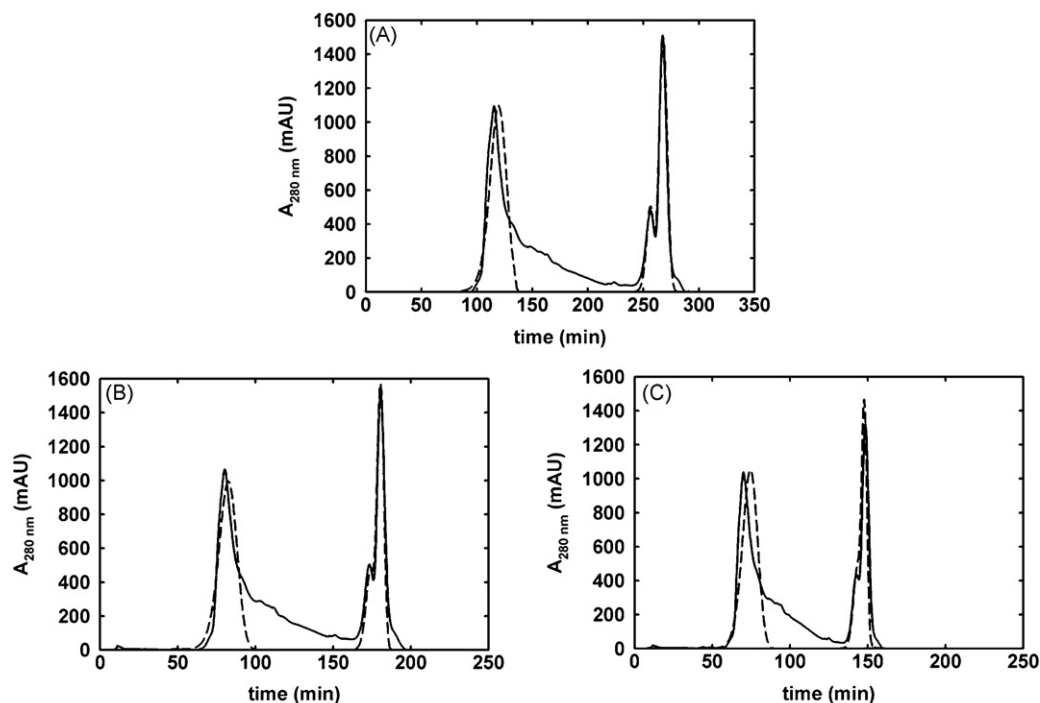
Fig. 8. Validation of the calculation of the model parameters through the comparison of experimental (—) and predicted (- - -) chromatograms from runs on Sepharose High Performance XK16; 40 ml laboratory columns. The elution profiles of a protein solution containing 7.50 mg ml^{-1} BSA and 2.50 mg ml^{-1} lactoferrin are obtained by loading the column with 0.4 column volumes, washing it with 2 column volumes, and eluting by increasing the concentration of the elution buffer from 0% to 100% over 10 column volumes. Following elution the column was washed with 2 column volumes of elution buffer without changing the fluid velocity. The column was loaded and washed at 100 cm h^{-1} whereas it was eluted at three different fluid velocities; 50 cm h^{-1} (A), 75 cm h^{-1} (B) and 100 cm h^{-1} (C). The values of model parameters have been calculated from the chromatograms in Fig. 7.

in charge gives rise to slight differences in elution conductivities on ion-exchange resins. Hence in this case where the resin was able to resolve these lactoferrin components the simulation was expanded to three components in order to model the additional lactoferrin peak.

The higher resolution of SP Sepharose High Performance in comparison with Capto S and SP Sepharose Fast Flow can be largely attributed to the differences in bead sizes. Specifically, the average bead size in SP Sepharose High Performance resin is 34 μm whereas it is 90 μm in Capto S and Sepharose Fast Flow matrices. Smaller beads give rise to larger numbers of theoretical plates and shorter diffusion distances into the porous beads and therefore less mass transfer restriction. Consequently, this gives elution profiles with higher resolution. The fitted parameters (adsorption/desorption kinetic parameters and effective diffusivity in the bead) for the SP Sepharose High Performance are independent of the bead size and consequently are similar to those of the SP Sepharose Fast Flow as both resins have similar material properties (Table 6).

The hydrodynamic radius of BSA and lactoferrin (BSA: 3.6 nm [28]; lactoferrin: 3.3 nm [29]) is much smaller than the size of the pores of the resins (~25 nm average pore radius for SP Sepharose Fast Flow resin; ~12 nm average pore radius for dextran coated resins) [16,21,24]. Additionally, foulants are not present to block the pores as the loading material is a solution of pure proteins. Therefore, the loading/elution of the proteins is expected to be dependent more on the maximum capacity and the kinetics of adsorption/desorption than on the effective diffusivity in the beads.

The main goal of this study was to predict the position and shape of the elution profiles obtained in laboratory and manufacturing scale columns using scale-down experimentation. Three types of matrices were used in order to test the generality of the approach. The peak positions were estimated with good accuracy for both laboratory and manufacturing scale runs with small differences to

be attributed to experimental variability (Tables 2–4). The shape of the predicted chromatograms gave consistently good predictions of the experimental results at all scales despite the existence of protein heterogeneity in both the BSA and lactoferrin. This makes it clear that accurate scale-up from 1 ml columns to 160 L is feasible.

5. Conclusions

Laboratory and manufacturing scale separation of a protein solution was predicted by inserting to the model the values for effective diffusivity, kinetic constants of adsorption/desorption and maximum capacity which were estimated from 1 ml column data using the genetic algorithm. Three types of matrices were used in order to test the generality of the model and performance during scale-up. The methodology follows QbD principles whereby process understanding was demonstrated.

Laboratory and manufacturing scale predictions were in good agreement with the experimentally obtained chromatographic data. The simulations provide process understanding of the underlying parameters controlling the separation.

The system used in this study is based on two proteins. Heterogeneity in these proteins increases the separation difficulty and hence the modelling and scale-up challenge, nevertheless the system is simplified in comparison to crude bioprocess materials. The use of the current empirical equations for axial dispersion and film mass transfer coefficient may be not sufficient for such feeds. A possible improvement in this study could be the experimental estimation and the development of new empirical equations to describe more complex materials.

Future work will be based on using representative bioprocess materials which contain a significant number of contaminants. These can interact with the column resin leading to competitive adsorption/desorption kinetics and mass transfer effects within the

column particularly under conditions of high loading which will make the prediction of chromatographic separations even more challenging.

Nomenclature

A_s	asymmetry factor
c_{bi}	concentration of component i in the mobile phase $(\mathrm{mg\,ml^{-1}})$
$c_{bi,inlet}$	inlet concentration $(\mathrm{mg\,ml^{-1}})$
c_{pi}	concentration of the component i in the liquid phase inside the beads $(\mathrm{mg\,ml^{-1}})$
$c_{pi,r=R_p}$	concentration of component at the surface of the bead $(\mathrm{mg\,ml^{-1}})$
D_{ax}	dispersion coefficient $(\mathrm{cm^2\,s^{-1}})$
D_M	molecular diffusivity of component i in water $(\mathrm{cm^2\,s^{-1}})$
D_{pi}	molecular diffusivity of component i in the liquid phase of the beads $(\mathrm{cm^2\,s^{-1}})$
$k_{ads,i}$	adsorption coefficient $(\mathrm{ml\,mg^{-1}\,s^{-1}})$
$k_{ads0,i}, k_{des0,i}$	phase modulators constants of the Langmuir kinetics $(\mathrm{ml\,mg^{-1}\,s^{-1}})$
$k_{des,i}$	desorption coefficient $(\mathrm{s^{-1}})$
k_i	mass transfer coefficient for the component $i\,(\mathrm{cm\,s^{-1}})$
L	length of the column (cm)
M	molecular weight (Da)
q_i	concentration of component i in the stationary phase $(\mathrm{mg\,ml^{-1}}$ solid phase)
$q_{max,i}$	maximum concentration of component i in the stationary phase $(\mathrm{mg\,ml^{-1}}$ solid phase)
Pe	Peclet number
r	radial coordinate (cm)
R_p	average bead radius (cm)
S	concentration of the salt in the elution buffer $(\mathrm{mg\,ml^{-1}})$
t	time (s)
v_{int}	interstitial velocity $(\mathrm{cm\,s^{-1}})$
z	axial coordinate (cm)

Greek symbols

β_i	constant which characterises the ion-exchange
γ_i	constant which characterise hydrophobic interactions $(\mathrm{ml\,mg^{-1}})$
ε_b	bed void volume fraction
ε_p	accessible particle void fraction

References

[1] International conference on harmonization (ICH) of technical requirements for registration of pharmaceuticals for human use, ICH harmonized guideline Q8(R2): Pharmaceutical Development, Step 4, August 2009.
[2] A.S. Rathore, H. Winkle, Nat. Biotechnol. 27 (2009) 26.
[3] N.J. Titchener-Hooker, P. Dunnill, M. Hoare, Biotechnol. Bioeng. 100 (2007) 473.
[4] N. Hutchinson, S. Chhatre, H. Baldascini, J.L. Davies, D.G. Bracewell, M. Hoare, Biotechnol. Progr. 25 (2009) 1103.
[5] W.R. Melander, S. El Rassi, C. Horváth, J. Chromatogr. 469 (1989).
[6] G. Guiochon, A. Felinger, D.G.G. Shirazi, Fundamentals of Preparative and Nonlinear Chromatography, second ed., Academic Press, 2006.
[7] V. Natarajan, W. Bequette, S.M. Cramer, J. Chromatogr. A 876 (2000) 51.
[8] J.M. Mollerup, T.B. Hansen, S. Kidal, A. Staby, J. Chromatogr. A 1177 (2008) 200.
[9] N. Jakobsson, D. Karlsson, J.P. Axelsson, G. Zacchi, B. Nilsson, J. Chromatogr. A 1063 (2005) 99.
[10] N. Forrer, A. Butté, M. Morbidelli, J. Chromatogr. A 1214 (2008) 59.
[11] P. Forssén, R. Arnell, T. Fornstedt, Compos. Chem. Eng. 883 (2006) 1381.
[12] D. Antos, W. Piatkowski, K. Kaczmarski, J. Chromatogr. A 874 (2000) 1.
[13] C.A. Orellana, C. Shene, J.A. Asenjo, Biotechnol. Bioeng. 104 (2009) 572.
[14] A. Jungbauer, O. Kaltenbrunner, Biotechnol. Bioeng. 52 (1996) 223.
[15] E.J. Suda, K.E. Thomas, T.M. Pabst, P. Mensah, N. Ramasubramanyan, M.E. Gustafson, A.K. Hunter, J. Chromatogr. A 1216 (2009) 5256.
[16] P. De Philips, A.M. Lenhoff, J. Chromatogr. A 883 (2000) 39.
[17] T. Gu, Mathematical modeling and scale-up of liquid chromatography, Springer, Berlin, 1995.
[18] E.J. Wilson, C.J. Geankoplis, Ind. Eng. Chem. Fundam. 5 (1966) 9.
[19] A. Polson, J. Phys. Colloid Chem. 54 (1950) 649.
[20] C.E. Schwartz, J.M. Smith, Ind. Eng. Chem. 45 (1953) 1209.
[21] B.D. Bowes, H. Koku, K.J. Czymmek, A.M. Lenhoff, J. Chromatogr. A 1216 (2009) 7774.
[22] T. Vicente, J.P. Mota, C. Peixoto, P.M. Alves, M.J. Carrondo, J. Chromatogr. A 1217 (2010) 2032.
[23] H.A. Chase, J Chromatogr. 291 (1984) 179.
[24] M.C. Stone, Y. Tao, G. Carta, J. Chromatogr. A 1216 (2009) 4465.
[25] B.C. To, A.M. Lenhoff, J. Chromatogr. A 1205 (2008) 46.
[26] J. Hubbuch, T. Linden, E. Knieps, A. Ljunglöf, J. Thömmes, M. Kula, J. Chromatogr. A 1021 (2003) 93.
[27] H. Wakabayashi, K. Yamauchi, M. Takase, Int. Dairy J. 16 (2006) 1241.
[28] P.M. Boyer, J.T. Hsu, Am. Inst. Chem. Eng. J. 38 (1992) 259.
[29] W.R. Bowen, X.W. Cao, P.M. Williams, Proc. R. Lond. Soc. Ser. A 455 (1999) 2933.